Supporting Information for "Global wave height trends and variability from new multi-mission satellite altimeter products, reanalyses and wave buoys"

B. W. Timmermans[1], C. P. Gommenginger[1], G. Dodet[2]and J-R Bidlot[3]

[1]National Oceanography Centre, European Way, Southampton SO14 3ZH, United Kingdom

[2]Laboratoire d'Océanographie Physique et Spatiale (LOPS), CNRS, IRD, Ifremer, IUEM, Univ. Brest, France

[3]European Centre for Medium-Range Weather Forecasts, Shinfield Road, Reading RG2 9AX, United Kingdom

Contents of this file

Text S1. Wave buoy data processing

Wave height data were obtained from buoys maintained by the U.S National Data Buoy Centre from the National Oceanographic and Atmospheric Administration (https://www.ndbc.noaa.gov/). In this study, analyses are limited to data buoys 46006 (eastern North Pacific) and 41002 (western North Atlantic). These wave buoys typically provide observations of significant wave height at hourly intervals. The published observations are not quality controlled, such that spurious and missing data can occur. Data loss from technical failure can result in an extended period of continuous data loss. In the absence of recommended quality control procedures, quality control is largely down to individual choice (e.g. Bidlot, Holmes, Wittmann, Lalbeharry, and Chen (2002); Caires and Sterl (2003); Gemmrich, Thomas, and Bouchard (2011)) and therefore highly variable.

Time series of Hs measurements from wave buoys were generated for comparison with gridded altimeter and simulation products. The buoy data were processed to derive monthly and annual mean Hs. Quality control included checks to ensure each monthly or annual mean contains sufficient data to be representative of the relevant period. Applied criteria included: i) a valid day comprises a minimum of 8 hourly observations; ii) a valid month comprises a minimum of 12 valid daily observations, and; iii) a valid year comprises at least 10 valid months.

In practice, missing data tend to occur for extended continuous periods of time (sometimes many months), presumably linked to technical faults or maintenance schedules. Therefore points (ii) and (iii) become the most onerous conditions in terms of data loss. Other data problems, such as anomalously high or low Hs values, were not frequently encountered, or were removed as part of the above procedure.

Text S2. Regression methods

In this paper, temporal trends are estimated primarily using simple linear regression applied to seasonal mean Hs, the emphasis of this analysis being on assessing different products with the same consistent methodology, rather than investigating different estimation methods, their effectiveness or absolute accuracies. Linear temporal trends are estimated by applying univariate linear regression models assuming normally distributed errors, and taking the regression slope coefficient as the trend. Important assumptions in this case are of zero or low temporal correlation and Gaussian distributed errors, and we have found these to be approximately satisfied.

The choice of regression method is important however, and the literature offers a vast range of different statistical approaches of varying complexity. Similar studies often employ the Sen slope method (Sen, 1968)—a non-parametric approach that provides more robust trend estimates when data have non-normal long-tailed distributions, offering improved robustness against outliers. Within the scope of our analysis, we applied the linear and Sen methods to annual mean Hs from buoys (Figure 2, main paper) and seasonal means from CCI2019 (Figure S3, this document) and found little difference in estimated trends. Importantly, while small differences can be found between the two methods, in our particular case, the trend differences are generally much larger between products than between regression methods.

A rigorous estimation of temporal trends in sea state was presented by Young and Ribal (2019) who applied a Seasonal Mann-Kendall test with Sen slope trend estimation (Hirsch et al., 1982). This non-parametric regression method evaluates trends systematically for individual months, then calculates the median slope across all months. The method accounts explicitly for serial dependence in data with strong seasonal components and provides estimates of significance, but provides a single estimate of trends averaged over all seasons. In this respect, our approach differs from that of Young and Ribal (2019) by estimating trends for individual seasons, and revealing interesting differences in trends between seasons in some locations (Figure S3).

Text S3. Confidence estimation

In this paper, estimates of statistical confidence are provided for the seasonal mean climatological differences (Figure S2) and the temporal trends (Figures 3 and S4). The robustness of the climatological mean differences (Figure S2) was estimated using a standard permutation bootstrap method (see e.g. Hesterberg (2011)), in this case with 3000 iterations. The statistical significance at the 10% level is estimated, on a 2×2 grid to ensure enough seasonal samples in each grid cell and to facilitate graphical presentation (small black dots in Figure S2). Statistical significance estimates for trends in Figures 3 and S4 are provided by the regression method, and is again depicted as black dots in relevant grid cells.

Statistical significance is frequently used in the literature to give a sense of robustness. It is standard practice, indeed quasi-compulsory, for publication. But statistical significance can also give a false sense of confidence since interpretation can be complicated by many issues. In this particular instance, both climatologies and trends are likely affected by a number of complications, e.g. the long-term reliability of the buoy data used quasi-universally (but in different ways) for satellite and model calibration; the differences between products in quality-control, calibration and filtering; and, the sensitivity to the choice of time period, noting the short observational record and substantial seasonal, interannual and decadal variability in many locations. Recognising these complexities, we provide estimates of confidence for the sake of consistency with other similar studies, but avoid making strong statements about trend robustness until the impact of important differences between the products is better understood. Instead, we encourage readers to note the marked differences seen between products in the spatial distributions of the seasonal mean Hs and trends in Figures 1/S1, S2 and 3/S4.

References

Bidlot, J.-R., Holmes, D. J., Wittmann, P. A., Lalbeharry, R., & Chen, H. S. (2002). Intercomparison of the performance of operational ocean wave forecasting systems with buoy data. *Weather and Forecasting*, *17*, 287-310.

Bidlot, J.-R., Lemos, G., & Semedo, A. (2019). *ERA5 reanalysis and ERA5-based ocean wave hindcast.* Retrieved from http://www.waveworkshop.org/16thWaves/Presentations/R1%20Wave_Workshop_2019_Bidlot_et_al.pdf

Caires, S., & Sterl, A. (2003). Validation of ocean wind and wave data using triple collocation. *Journal of Geophysical Research*, *108*. doi: 10.1029/2002JC001491

Gemmrich, J., Thomas, B., & Bouchard, R. (2011). Observational changes and trends in northeast Pacific wave records. *Geophysical Research Letters*, *38*. doi: 10.1029/2011GL049518

Hersbach, H., de Rosnay, P., Bell, B., Schepers, D., Simmons, A., Soci, C., ... Zuo, H. (2018, December). *Operational global reanalysis: progress, future directions and synergies with NWP* (Tech. Rep.). European Centre for Medium Range Weatherforecasting. Retrieved from https://www.ecmwf.int/en/elibrary/18765-operational-global-reanalysis-progress-future-directions-and-synergies-nwp doi: 10.21957/tkic6g3wm

Hesterberg, T. (2011). Bootstrap. *Wiley Interdisciplinary Reviews: Computational Statistics*, *3*(6), 497–526. doi: 10.1002/wics.182

Hirsch, R. M., Slack, J. R., & Smith, R. A. (1982). Techniques of trend analysis for monthly water quality data. *Water Resources Research*, *18*, 107-121. doi: 10.1029/WR018i001p00107

Piollé, J.-F., Dodet, G., & Quilfen, Y. (2020c). *ESA Sea State Climate Change Initiative : Global remote sensing merged multi-mission monthly gridded significant wave height, L4 product, version 1.1., Centre for Environmental Data Analysis.* Retrieved from `http://dx.doi.org/10.5285/47140d618dcc40309e1edbca7e773478` doi: 10.5285/47140d618dcc40309e1edbca7e773478

Sen, P. K. (1968). Estimates of the regression coefficient based on Kendall's Tau. *Journal of the American Statistical Association*, *63*, 1379-1389. doi: 10.1080/01621459.1968.10480934

Young, I. R., & Ribal, A. (2019). Multiplatform evaluation of global trends in wind speed and wave height. *Science*, *364*, 548-552. doi: 10.1126/science.aav9527

Table S1. Summary of sea state products used for analysis

Data set	Variables used	Resolution (spatial)	Resolution (temporal)	Details [Period used]
CCI Level 4	Mean Hs	1.0 deg.	Monthly	[1992-2017]
(Piollé et al., 2020c)				Excludes Sentinel-3A, JASON 3
Ribal and Young (RY2019)	Hs from Ku-band, 1 Hz measurements	Along-track	Continuous	[1992-2017]
				Excludes Sentinel-3A, JASON 3, SARAL-AltiKa
ERA5 (ECMWF)	Mean Hs	0.5 deg.	Monthly	[1980-2018]
(Hersbach et al., 2018)				
ERA5 hindcast (CY46R1)	Mean Hs	0.5 deg.	Monthly	[1980-2018]
(Bidlot et al., 2019)				

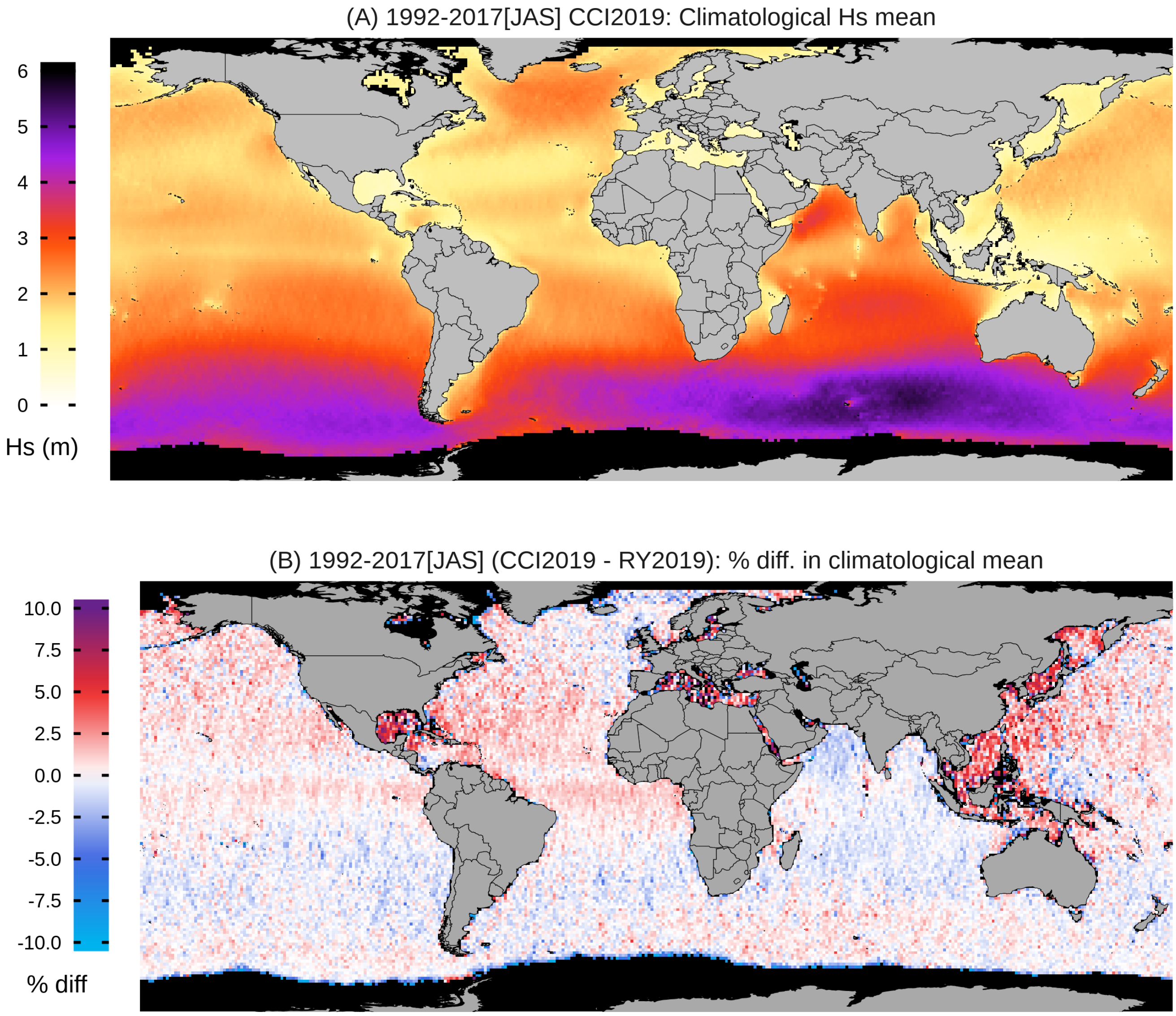

Figure S1. (A) Global climatological JAS mean Hs computed on a $1° \times 1°$ grid over 1992-2017 for CCI2019 product. (B) Difference (%) between climatological mean Hs from CCI2019 and RY2019.

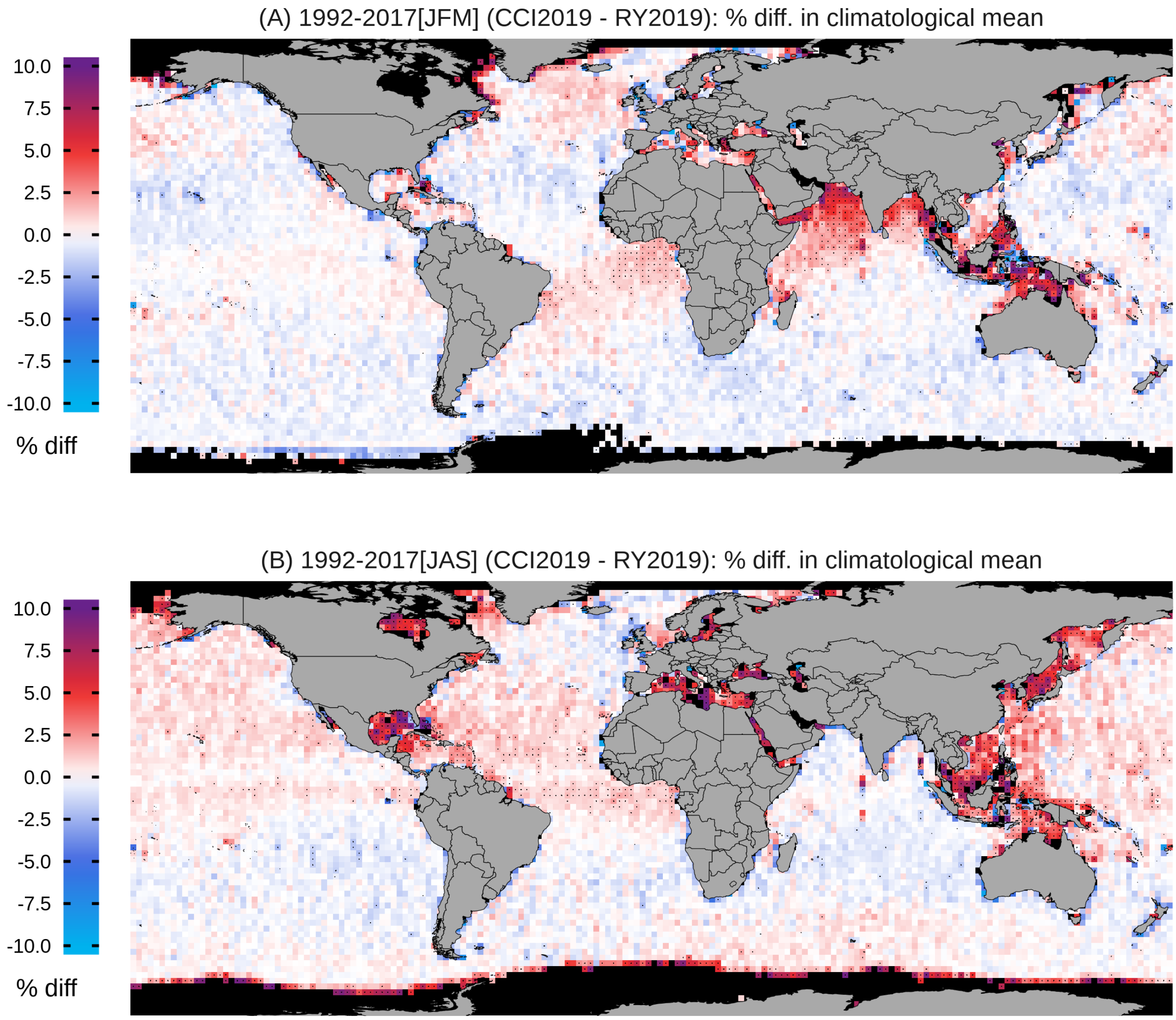

Figure S2. (A) Difference (%) between climatological JFM mean Hs from CCI2019 and RY2019. (B) Difference (%) between climatological JAS mean Hs from CCI2019 and RY2019. Shown on a $2^\circ \times 2^\circ$ grid. Dots indicate grid cells with mean differences significant at the 10% level, based upon a bootstrap method for the monthly means.

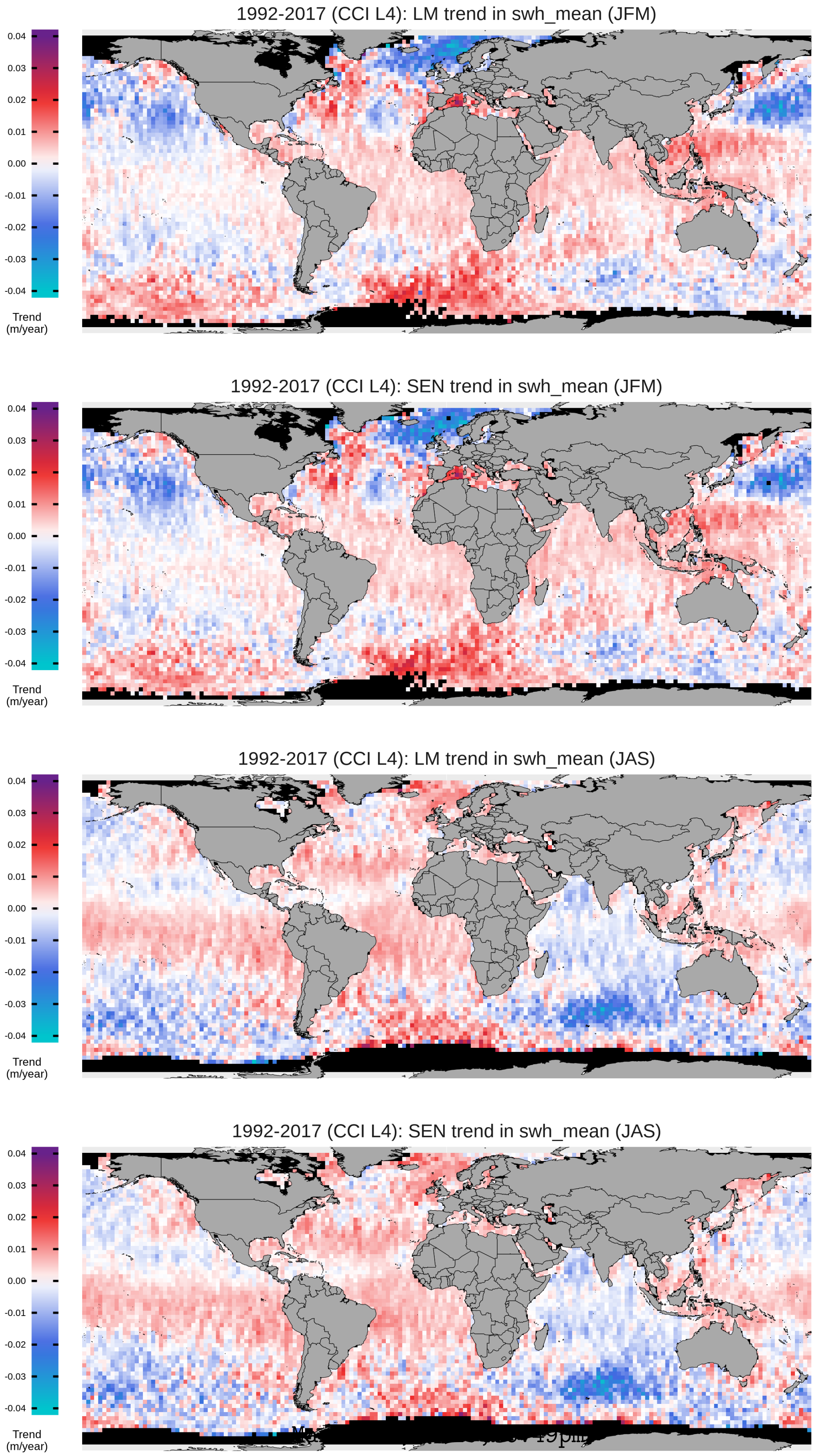

Figure S3. Global distribution of mean Hs trend estimates for JFM (top two panels) and JAS (bottom two panels) on a $2° \times 2°$ grid over 1992-2017 for CCI2019 product obtained with linear regression (panels 1 & 3) and Sen slope methods (panels 2 & 4).

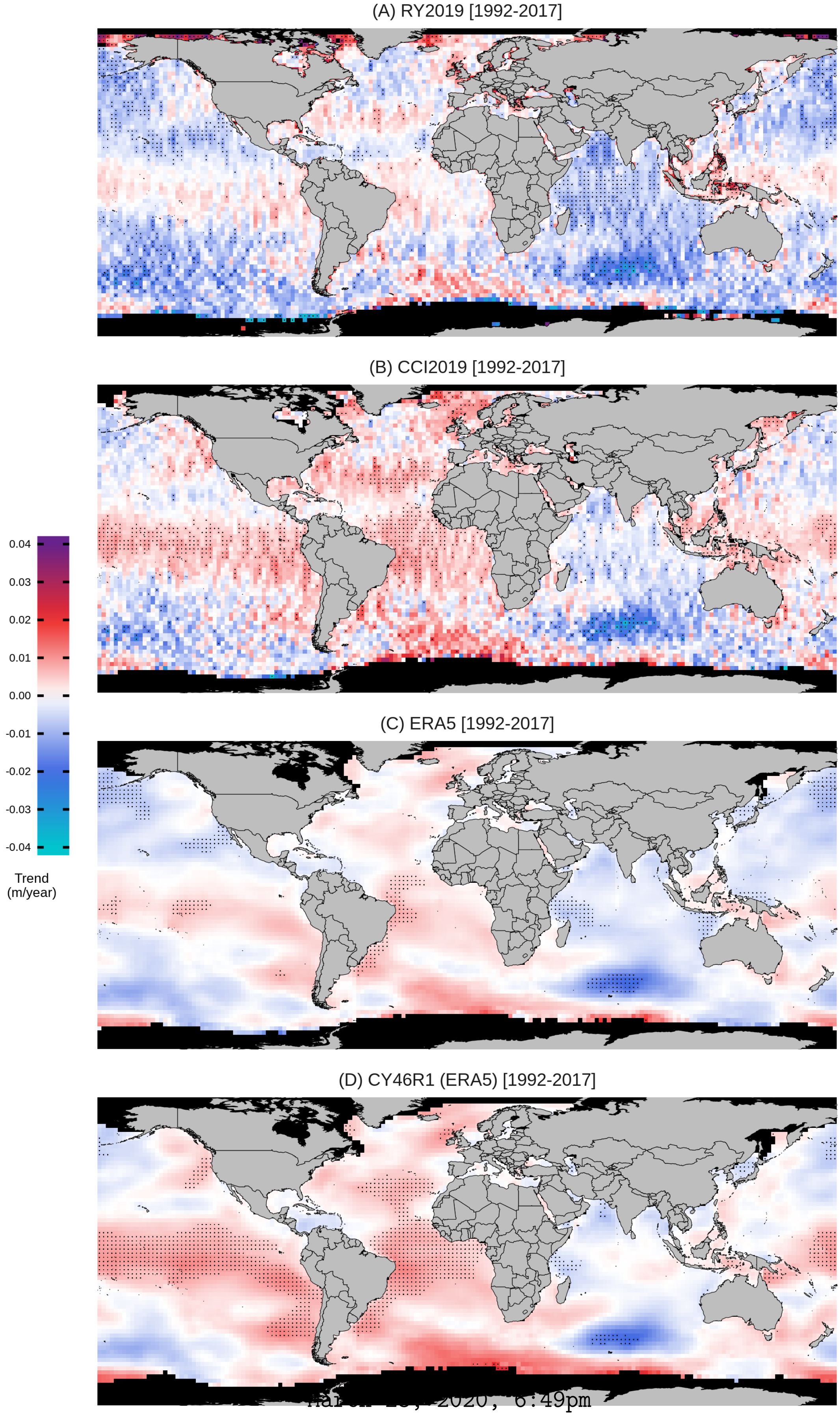

Figure S4. Global distribution of JAS mean Hs trend estimates on a $2° \times 2°$ grid over 1992-2017 for (A) RY2019, (B) CCI2019, (C) ERA5 and (D) CY46R1. Dots indicate grid cells where the trend coefficient is significant at the 5% level.